

Insights into the fluoride ions response mechanism for the novel 2,2':6',2''-terpyridine fluorescent sensor

Received Oct. 18, 2017,
Accepted Nov. 29, 2017,

DOI: 10.4208/jams.101817.112917a

<http://www.global-sci.org/jams/>

Xuemei Lu^a, Yuchuan Zhai^{a,*} and Meixia Zhang^{b,*}

Abstract. In this present work, the sensing mechanism of a novel fluoride chemosensor 2,2':6',2''-terpyridine (abbreviated as "2" according to previous experiment) has been investigated based on density functional theory (DFT) and time-dependent DFT (TDDFT) methods. The theoretical electronic spectra (vertical excitation energies and fluorescence peak) reproduced previous experimental results [*RSC Adv.* **2014**, *4*, 4041.], which confirms the rationality of our theoretical level used in this work. The constructed potential energy curve suggest that the non-barrier process could be responsible for the rapid response to fluoride anion. Analyses about binding energies demonstrate that only fluoride anion could be detected for 2 chemosensor in acetonitrile solvent. Comparing with other anions, we confirm the uniqueness of fluoride anion for 2 sensor. In view of the excitation process, the strong intramolecular charge transfer (ICT) process of $S_0 \rightarrow S_1$ transition explain the redshift of absorption peak for 2 sensor with the addition of fluoride anion. This work not only presents a straightforward sensing mechanism of fluoride anion for 2 chemosensor, but also plays important roles in synthesizing and designing fluorescent sensors in future.

1. Introduction

As the smallest anion owning the unique position among all the essential anions, fluoride anion (F^-) plays an important role in many ranges about chemical and biological fields [1-3]. In fact, even though fluoride ion is beneficial to dental health and treatment of osteoporosis [4], obvious fluoride toxicity can be generally exposed on a less salubrious level to lead to fluorosis in terms of increasing bond density, urolithiasis, and even cancer [5]. Therefore, it has become the high demand to make considerable effects in detecting and recognizing fluoride anions. And lots of attention has been focused on the selective sensing for fluoride ions recently [6-9]. Particularly, it is important to develop novel optical probes revealing high selectivity, good sensitivity and rapid response toward fluoride anions [10-15].

In general, for developing ideal fluoride anion probes, the following characters could be considered. For more legible, it should be the best choice for presenting apparent optical signal modifies to realize the naked-eye detection [16]. It will be better to own optical signals from far-red to near-infrared region to avoid interference from endogenous sensors in biological system [17]. Showing practical applications of detecting fluoride in real samples is also another attractive aspect [18]. To the best of knowledge, at present, the strategies for constructing fluoride probes are mostly based on B-F complexation, F-induced desilylation of Si-O bands and deprotonation via hydrogen bond [19-25]. And generally, the fluorescence transduction processes are involved in photoinduced electron transfer (PET), intramolecular charge transfer (ICT), excited state proton transfer (ESPT), and so on [26-29]. In fact, although more and more work about fluoride anion have been reported, theoretical investigations about fluoride-sensing mechanisms are

rare relatively.

Recently, Cao *et al.* synthesized two novel fluorescent sensors (named as 1 and 2 according to experiment) experimentally [30]. They found that the both 1 and 2 sensors show the colorimetric and luminescent response to the fluoride anion over other anions based on strong hydrogen bonding interaction ($O-H\cdots F$) in organic solvent. And upon the addition fluoride anions, these two receptor can show the color change from colorless to yellow. In fact, the probe response mechanism of compound 1 could be understood clearly, which can be attributed to that the ESPT process could be inhibited by the fluoride anions [19, 21, 26]. Whereas for sensor 2,2':6',2''-terpyridine (abbreviated as "2" according to previous experiment), the response mechanism seems to be scarce theoretically. To the best of our knowledge, just the indirect information about structural and photochemical properties could be provided in experimental studies. While the calculations of electronically excited states can be adopted to clarify the fundamental aspects about

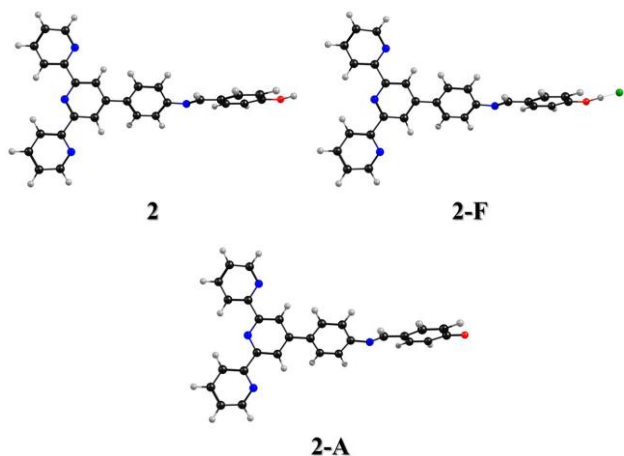


Figure 1: View of the relative structures of 2, 2-F and 2-A. Herein, black: C atoms; gray: H atoms; Blue: N atoms; Red: O atoms; Green: F atom.

^a School of metallurgy, Northeastern University, Shenyang, 110819, E-mail: zhaiyc@smm.neu.edu.cn

^b Department of Physics, Liaoning University, Shenyang, 110036, E-mail: ldxmx@sina.com

sensing mechanism. Particularly, the mechanism about “on-off” process is the fundamental aspects of 2, which might be useful for understanding and controlling probe response about 2 and its derivatives in future.

In this present work, therefore, the density functional theory (DFT) and time-dependent density functional theory (TDDFT) methods have been adopted to investigate the fluoride sensing performances and the relative mechanism for 2 sensor. On the basis of Kasha’s rule [31], fluorescence radiation happens with an electron relaxes from S_1 state to its S_0 state, therefore, both S_0 and S_1 states of 2 and relative structures are of interest in this work. Based on comparing the structural parameters and reaction energies with other anions, we clarify the ability of F⁻ for 2 sensor. Particularly, we mainly focus our attention on the changes of photochemical properties and the excited-state charge redistributions upon adding the fluoride anion. Comparing with other anions, we confirm the uniqueness of fluoride anion. We deem the mechanism we put forward is very important for the synthesis and design for fluorescent sensors in future.

2. Theoretical Methods

In this work, all the simulated calculations have been carried out using Gaussian 09 program [32]. Within the framework of DFT and TDDFT methods, the hybrid exchange-correlation functional B3LYP and the triple- ζ valence quality with one set of polarization functions (TZVP) basis set have been selected in all calculations [33-39]. In view of the solvent effect, acetonitrile (the dielectric constant: 35.688) solvent has been adopted within the model of Polarizable Continuum Model (PCM) using the integral equation formalism variant (IEFPCM) [40-42], which considers the solute in the cavity of overlapping solvent that own apparent charges to reproduce the electrostatic potential because of the polarized dielectric within the cavity. The ground-state geometries for all the species have been optimized without constraint. And the vibrational frequencies have been also analyzed at the optimized structures to ensure these structures corresponded to the local minima on the S_0 state potential energy surface. The vertical excited energies have been performed from the ground state stable form using TDDFT, and six low-lying excited states are predicted in this work. The excited-state structures have been calculated starting from the S_0 -state stable configuration with analyzing vibrational frequencies to confirm the stability. The calculations about potential energy curves for the probe response process have been also carried out to explain the mechanism. All the stationary points along with reaction coordinate were optimized in acetonitrile solvent. Analyses of frequency can obtain the thermodynamic corrections in the corresponding electronic states. Zero-point energy correction and

thermal corrections to the Gibbs free energy were also performed according to the harmonic vibrational frequencies.

Fine quadrature grids of size 4 were employed. The self-consistent field (SCF) convergence thresholds of the energy for both the ground state and excited state optimization were set at 10^{-8} (default settings are 10^{-6}). Harmonic vibrational frequencies in the ground and excited state were determined by diagonalization of the Hessian. The excited-state Hessian was obtained by numerical differentiation of the analytical gradients using central differences and default displacements of 0.02 Bohr. The infrared intensities were determined from the gradients of the dipole moment.

3. Results and discussion

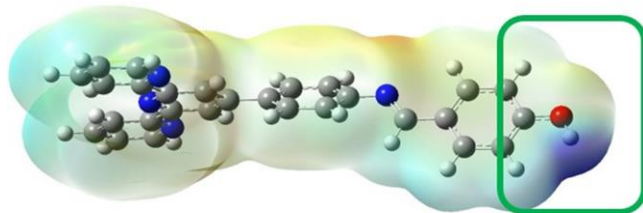
The geometries of the chemosensor 2, the fluoride complex 2-F form and the anion product 2-A structure have been optimized based on the B3LYP/TZVP theoretical level within the framework of the IEFPCM solvent model (see Figure 1). In the process of investigating the possible correlation of electrostatic potential with hydrogen bonding interactions (shown in Figure 2), the regions of the negative electrostatic potential (denoted by red) are usually used to identify the hydrogen bond acceptor sites. Whereas for describing the hydrogen bond donating sites, the regions of positive potential (denoted by blue) are prominent [29]. Obviously, the positive electrostatic potential around H atom of oxhydryl exists in 2 chemosensor. The corresponding natural bond orbital (NBO) charge analyses also reveal that the hydrogen atom should be the most possible reactive site of 2 sensor for attracting fluoride ion. Therefore, the fluoride complex 2-F form can be reasonably obtained via optimizing corresponding stable structure. And for complex 2-F, a relatively effective method (i.e., the quantum theory of atoms in molecules (AIM)) was used in this work to investigate hydrogen bonds of the normal DOX configuration in the S_0 state. Given the AIM theory, identification of a critical point (CP) and the existence of a bond path in equilibrium geometry are necessary and sufficient conditions for assigning an interaction between two primary atoms [43]. And the AIM analysis of the title compounds ensure the presence of an appreciable interaction in between the atoms concerned. The relevant AIM topological parameters involved in the optimized geometries show that the $p(r)$ at the bond critical point (BCP) for the S_0 -state 2-F geometry is around 0.037 a.u. respectively, which is close to the 0.040 a.u. (the maximum threshold value proposed by Popelier to ensure the presence of hydrogen bond [44]). It justifies the presence of intermolecular hydrogen bonds ($O-H\cdots F$), which is further substantiated from the corresponding $\nabla^2 p_c$ value (0.124) being well within the range (0.02 ~ 0.15 a.u.) [43, 44]. Therefore, it can be further demonstrated that hydrogen bond should be formed for 2-F in the S_0 state.

One thing is interesting that the fluoride anion-added deprotonation forming 2-A form via hydrogen bond can be used to interpret this kind of response mechanism of fluoride ion probe as mentioned in experiment [30], however, why other anions could

Table1: The theoretical binding energies (kcal/mol) for 2 chemosensor with different anions using the B3LYP/TZVP theoretical level in acetonitrile solvent

F	Cl	Br	$H_2PO_4^-$	CH_3COO^-	CN ⁻	HSO_4^-	ClO_4^-	NO_3^-
21.54	8.49	6.48	6.05	6.49	8.46	7.38	9.51	8.14

Figure 2: View of the electrostatic potential surface of 2 sensor in the S_0 state.



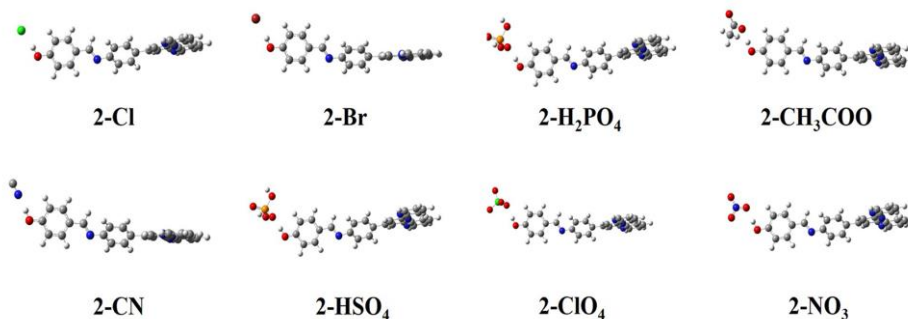


Figure 3: View of the structures of 2-Cl, 2-Br, 2-H₂PO₄, 2-CH₃COO, 2-CN, 2-HSO₄, 2-ClO₄ and 2-NO₃ complexes based on B3LYP/TZVP theoretical level in the S₀ state.

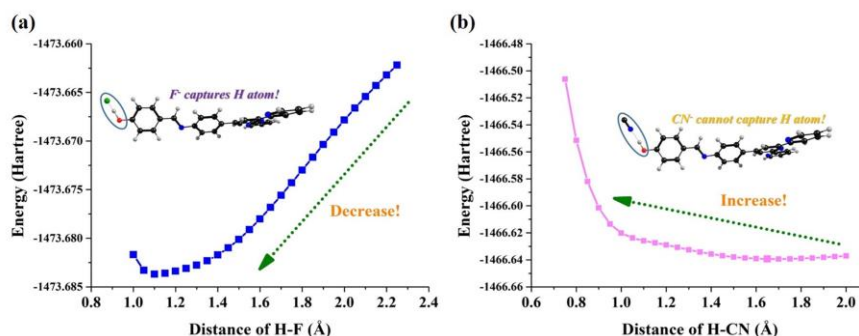


Figure 4: The constructed potential energy curves of S₀ state for 2 chemosensor with the addition of fluoride anion and CN anion.

not lead to response? With this kind of doubt, we also study other anions (Cl⁻, Br⁻, H₂PO₄⁻, CH₃COO⁻, CN⁻, HSO₄⁻, ClO₄⁻ and NO₃⁻) combining with 2 sensor. The relative structures of these complexes have been displayed in Figure 3. The investigations about binding energies between 2 chemosensor itself and the anions could be reasonable for explaining the high selectivity of fluoride anion. Particularly, this manner can reasonably show why just the fluoride anion can be detected in previous experiment [30]. All the optimizations about these complexes have been performed based on DFT/B3LYP/TZVP IEFPCM (acetonitrile) theoretical level. For investigating the binding energies, we adopted the formula E_{binding} (ΔE) = E₂ + E_{Anion} - E_{Complex}. In addition, given the intermolecular interactions, we also used the basis set superposition error (BSSE) manner to calculate the binding energy. The calculated binding energies of corresponding anions have been listed in Table 1. It can be clearly seen that the binding energy between the fluoride anion and 2 is the biggest one (21.54 kcal/mol), which is much larger than other anions. The addition of fluoride anion could interact with 2 via the most binding energy 21.54 kcal/mol 7 kcal/mol in the ground state, and the calculated H-F bond distance in 2 form is 0.99 Å, which is close to the length of HF molecule (0.92 Å) in gas [45].

In addition, in order to further reveal the effect of the fluoride triggered deprotonation process in the fluoride-sensing mechanism of 2 chemosensor, we also calculate the corresponding potential energy curves as shown in Figure 4 (a). The potential energy curve of S₀ state is based on the shortening of F and H atom of hydroxy from 2.30 Å to 1.00 Å with fixing the step of 0.05 Å, which has been confirmed to be a good manner to deal with the studies of protonated and deprotonated processes. It can be seen clearly that the potential energy curve almost decreases along with the shortening H-F bond length. That is to say, fluoride triggered deprotonation process occurs spontaneously forming 2-A configuration in the S₀ state. To explain why other anions could not be responded, herein,

we also take the CN⁻ as an example (see Figure 4 (b)). Similar with the calculated process of Figure 4 (a), the potential energy curve about shortening H-N distance has been constructed. The H-N distances in the S₀ state is from 2.00 to 0.80 Å in step of 0.05 Å. Obviously, the potential energy curve is increasing along with the shortened H-N distance, which indicates that the detection of CN⁻ for 2 systems is not exothermal. In other words, the deprotonation process could not proceed for CN⁻ and other anions.

The calculated frontier molecular orbitals for 2 and 2-A have been shown in Figure 5 to further explain the red shift with the addition of fluoride anion. The first permitted transitions for 2 and 2-A are from the highest occupied molecular orbital (HOMO) to the lowest unoccupied molecular orbital (LUMO) with oscillator strengths, respectively. Clearly, the S₀ → S₁ transition should be the ππ*-type characteristic. It can be seen that the O atom of 2 makes a considerable contribution to the HOMO orbital, while its contribution to LUMO is largely decreased. For the anion form 2-A form, it can be found that the intramolecular charge transfer (ICT) character is different from 2 one. More charges transfer to left region. Thus, for 2-A compound, the red shift about the absorbance

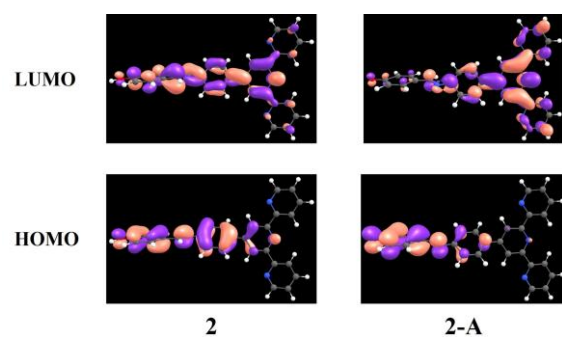


Figure 5: The calculated frontier molecular orbitals (HOMO and LUMO) for 2 and 2-A compounds based on TDDFT/B3LYP/TZVP theoretical level in acetonitrile solvent.

band should be ascribed to the ICT process via adding fluoride anions.

4. Conclusions

In summary, in this work, we theoretically explore the fluoride-sensing mechanism of 2 chemosensor based on DFT and TDDFT methods. We mainly focus our attention on the sensing process of fluoride anion and successfully explain why just fluoride ion can be detected uniquely. The addition of fluoride anion can spontaneously capture the hydrogen proton of hydroxyl forming intermolecular hydrogen bond O-H···F. Due to the exothermal deprotonation process for 2-F complex, the 2-A configuration can be formed in the S₀ state. While for other anions, the corresponding deprotonation process is endothermic. And the experimental steady-state absorption spectra have been well reproduced by our calculated vertical excitation energies. Particularly, because of the ICT process from the transition S₀ → S₁ in 2-A, the absorption peak of 2-A exhibits the red shift comparing with that of 2. We not only present the unambiguous sensing mechanism of fluoride anion, but also wish this mechanism can play roles in synthesizing and designing fluorescent sensors in future.

Acknowledgements

This work was financially supported by the Innovative Talent Support Program of Liaoning Province (Grant No. LR2017062), the Liaoning Provincial Department of Education Project (Grant No. LFW201710), the Natural Science Foundation of Liaoning Province (Grant No. 201601095 and 201602345), and the program of the Liaoning Key Laboratory of Semiconductor Light Emitting and Photocatalytic Materials.

References

- [1] M. Kleerekoper, *Endocrinol. Metab. Clin. North Am.* **1998**, *27*, 441.
- [2] P. Connell, *Fluoride*, **2007**, *40*, 155.
- [3] Y. M. Yang, Q. Zhao, W. Feng, F. Y. Li, *Chem. Rev.* **2013**, *113*, 192.
- [4] P. E. Rakita, *J. Chem. Educ.* **2004**, *81*, 677.
- [5] P. P. Singh, M. K. Barjatiya, S. Dhing, R. Bhatnagar, S. Kothari, V. Dhar, *Urol. Res.* **2001**, *29*, 238.
- [6] G. Saikia, A. K. Dwivedi, P. K. Iyer, *Anal. Methods* **2013**, *4*, 3180.
- [7] B. Ke, W. Chen, N. Ni, Y. Cheng, C. Dai, H. Dinh, B. Wang, *Chem. Commun.* **2013**, *49*, 2494.
- [8] L. Gai, H. Chen, B. Zou, H. Lu, G. Lai, Z. Li, Z. Shen, *Chem. Commun.* **2012**, *48*, 10721.
- [9] Y. Zhou, J. Zhang, J. Yoon, *Chem. Rev.* **2014**, *114*, 5511.
- [10] P. Song, J. X. Ding, T. S. Chu, *Spectrochimica Acta Part A* **2012**, *97*, 746.
- [11] J. S. Chen, R. Z. Liu, Y. Yang, T. S. Chu, *Theor. Chem. Acc.* **2014**, *133*, 1411.
- [12] P. Song, A. H. Gao, P. W. Zhou, T. S. Chu, *J. Phys. Chem. A* **2012**, *116*, 5392.
- [13] J. S. Chen, P. W. Zhou, L. Zhao, T. S. Chu, *RSC Adv.* **2014**, *4*, 254.
- [14] G. Li, P. Song, G. Z. He, *Chin. J. Chem. Phys.* **2011**, *24*, 305.
- [15] G. Y. Li, T. Chu, *Phys. Chem. Chem. Phys.* **2011**, *13*, 20766.
- [16] R. Hu, J. Feng, D. Hu, S. Wang, S. Li, Y. Li, G. Yang, *Angew. Chem., Int. Ed.* **2010**, *49*, 4915.
- [17] G. Patonay, M. D. Antoine, *Anal. Chem.* **1991**, *63*, 321.
- [18] Y. Jiang, X. Hu, J. Hu, H. Liu, H. Zhong, S. Liu, *Macromolecules* **2011**, *44*, 8780.
- [19] G. Y. Li, D. Liu, H. Zhang, W. W. Li, F. Wang, Y. H. Liang, *Spectrochimica Acta Part A* **2015**, *149*, 17.
- [20] X. Zheng, W. Zhu, D. Liu, H. Ai, Y. Huang, Z. Lu, *ACS Appl. Mater. Interaces* **2014**, *6*, 7996.
- [21] G. Y. Li, G. J. Zhao, K. L. Han, G. Z. He, *J. Comput. Chem.* **2011**, *32*, 668.
- [22] Z. Lou, P. Li, K. Han, *Acc. Chem. Res.* **2015**, *48*, 1358.
- [23] Z. Lou, S. Yang, P. Li, P. Zhou, K. Han, *Phys. Chem. Chem. Phys.* **2014**, *16*, 3749.
- [24] Z. Lou, P. Li, Q. Pan, K. Han, *Chem. Commun.* **2013**, *49*, 2445.
- [25] V. Amendola, G. Bergamaschi, M. Boiocchi, L. Fabbrizzi, L. Mosca, *J. Am. Chem. Soc.* **2013**, *135*, 6345.
- [26] G. Y. Li, G. J. Zhao, Y. H. Liu, K. L. Han, G. Z. He, *J. Comput. Chem.* **2010**, *31*, 1759.
- [27] Y. H. Liu, M. S. Mehata, S. C. Lan, *Spectrochimica Acta Part A* **2014**, *128*, 280.
- [28] Y. Li, J. Chen, T. S. Chu, *J. Lumin.* **2016**, *179*, 203.
- [29] Y. Li, T. S. Chu, *J. Phys. Chem. A* **2017**, *121*, 5245.
- [30] Q. Y. Cao, M. Li, L. Zhou, Z. W. Wang, *RSC Adv.* **2014**, *4*, 4041.
- [31] M. Kasha, *Discuss. Faraday Soc.* **1950**, *9*, 14.
- [32] M. J. Frisch, G. W. Trucks, H. B. Schlegel, G. E. Scuseria, M. A. Robb, J. R. Cheeseman, G. Scalmani, V. Barone, B. Mennucci, G. A. Petersson, H. Nakatsuji, M. Caricato, X. Li, H. P. Hratchian, A. F. Izmaylov, J. Bloino, G. Zheng, J. L. Sonnenberg, M. Hada, M. Ehara, K. Toyota, R. Fukuda, J. Hasegawa, M. Ishida, T. Nakajima, Y. Honda, O. Kitao, H. Nakai, T. Vreven, J. A. Montgomery Jr, J. E. Peralta, F. Ogliaro, M. Bearpark, J. J. Heyd, E. Brothers, K. N. Kudin, V. N. Staroverov, T. Keith, R. Kobayashi, J. Normand, K. Raghavachari, A. Rendell, J. C. Burant, S. S. Iyengar, J. Tomasi, M. Cossi, N. Rega, J. M. Millam, M. Klene, J. E. Knox, J. B. Cross, V. Bakken, C. Adamo, J. Jaramillo, R. Gomperts, R. E. Stratmann, O. Yazyev, A. J. Austin, R. Cammi, C. Pomelli, J. W. Ochterski, R. L. Martin, K. Morokuma, V. G. Zakrzewski, G. A. Voth, P. Salvador, J. J. Dannenberg, S. Dapprich, A. D. Daniels, O. Farkas, J. B. Foresman, J. V. Ortiz, J. Cioslowski, D. J. Fox, Gaussian 09, revision D.01; Gaussian, Inc., Wallingford, CT, **2009**.
- [33] C. Lee, W. Yang, R. Parr, *R. Phys. Rev. B* **1988**, *37*, 785.
- [34] B. Miehlich, A. Savin, H. Stroll, H. Preuss, *Chem. Phys. Lett.* **1989**, *157*, 200.
- [35] W. Kolth, A. Becke, R. Parr, *J. Phys. Chem.* **1996**, *100*, 12974.
- [36] S. Vosko, L. Wilk, M. Nusair, *Can. J. Phys.* **1980**, *58*, 1200.
- [37] O. Treutler, R. Ahlrichs, *J. Chem. Phys.* **1995**, *102*, 346.
- [38] F. Furche, R. Ahlrichs, *J. Chem. Phys.* **2002**, *117*, 7433.
- [39] D. Feller, *J. Comput. Chem.* **1996**, *17*, 1571.
- [40] B. Mennucci, E. Cancès, J. Tomasi, *J. Phys. Chem. B* **1997**, *101*, 10506.
- [41] E. Cancès, B. Mennucci, J. Tomasi, *J. Chem. Phys.* **1997**, *107*, 3032.
- [42] R. Cammi, J. Tomasi, *J. Comput. Chem.* **1995**, *16*, 1449.
- [43] P. Hobza, Z. Haylas, *Chem. Rev.* **2000**, *100*, 4253.
- [44] D. Kosov, P. Popelier, *J. Phys. Chem. A* **2000**, *104*, 7339.
- [45] D. Lide, CRC Handbook of Chemistry and Physics, 84th ed., CRC press, Cleveland, **2004**.